

Cytoskeleton con nement of red blood cell membrane uctuations

N. Gov, A. G. Zilman and S. Safran
 Department of Materials and Interfaces,
 The Weizmann Institute of Science,
 P.O.B. 26, Rehovot, Israel 76100

We analyze both the static and dynamic uctuation spectrum of the red-blood cell in a uni ed manner, using a simple model of the composite membrane. In this model, the two-dimensional spectrin network that forms the cytoskeleton is treated as a rigid shell which is located at some constant average separation from the lipid bilayer. The cytoskeleton thereby con nes both the static and dynamic uctuations of the lipid bilayer. The predictions of the model account for the wavevector and frequency dependence of the experimental data. The observed amplitude of the thermal uctuations is related to e ects of ATP-driven uctuations.

PACS numbers:

A long-standing problem in the study of red blood cell (RBC) structure is the simultaneous softness of its membrane observed by thermal uctuations [1], and the strong shear elasticity found in static deformation experiments, such as micropipette aspiration [2] and electrodeformation [3]. The membrane itself is a composite structure [4] with an outer, gel-like extracellular network of long sugar molecules (thought to be irrelevant to the structural strength), a mixed lipid/protein bilayer and an attached, intracellular network. Previous theoretical models of this membrane treated it as a single, polymerized network with the combined curvature bending modulus of the lipid bilayer and the shear rigidity of the cytoskeleton [5]. Such models were successful in describing the response of the membrane in static deformation experiments, which give $10^5 - 10^6 \text{ J/m}^2$ [2, 3, 6]. However, comparing these models to the uctuation data, leads to the conclusion that the membrane behaves as if the shear modulus vanishes $\rightarrow 0$ [5, 7]. This surprising conclusion comes from the shape and amplitude analysis of the longest wavelength shape uctuations [1, 8]. Various ideas have been raised in order to account for this observation, the main suggestion being that ATP-driven structural rearrangement in the spectrin network [1, 4, 6] relaxes the shear-like deformations.

The previous studies were concerned with the shape uctuations of largest wavelength. Here, we focus on the uctuation spectrum, at the length-scales of $1 - 0.1 \mu\text{m}$, where the e eect of the cytoskeleton is observed [9]. The important question is to what extent the cytoskeleton e ects are distinguishable from the uctuations of a free, closed bilayer. We show that for a consistent description of both the static and the dynamic uctuation spectrum we must include the con ninge ects of the cytoskeleton. A simple model where the only signi cant e eect of the spectrin network is to con ne the lipid bilayer membrane, consistently describes both the spatial and temporal spectra of the thermal uctuations of the RBC membrane. We discuss how active processes that e eectively increase the temperature of the membrane, can be accounted for within this description.

The curvature bending modulus of the lipid bilayer

[10] is deduced from measurements of the amplitude of thermal uctuations at the smallest measured wavelengths [9]: $\sim 2 - 10^{20} \text{ J}$. The RBC cytoskeleton is a two-dimensional, roughly triangular, network of spectrin proteins [11], that is attached to the lipid bilayer at the nodes and at additional, random sites along the spectrin polymers. The cytoskeleton is well described as a network of entropic springs, of length $l \sim 80 \text{ nm}$ [11, 12], with an e eective spring constant: $\sim 4 - 10^6 \text{ J/m}^2$, which is close to the measured static shear modulus: $\sim 6 - 10^6 \text{ J/m}^2$ [2]. Compared with the lipid bilayer bending modulus, the curvature bending modulus of the cytoskeleton is negligible [1, 13]: $\kappa_{\text{cyto}} \sim 10^{21} - 10^{22} \text{ J}$ for a cytoskeleton thickness of $w \sim 100 - 500 \text{ \AA}$.

We now begin by analyzing the measured spatial correlations of the uctuations [9], and describe the e ects of the cytoskeleton on the bilayer in terms of continuum mechanics. This is feasible since the cytoskeleton forms a rather open mesh that is attached to the bilayer at discrete points with a contact area that is small ($\sim 1 \text{ nm}^2$) compared to the inter-node distance ($\sim 100 \text{ nm}$). In a coarse grained picture, we can describe the thermal uctuations of the bilayer using a continuum model of the free energy functional

$$F = \int dS \left[\frac{1}{2} (\nabla h)^2 + \frac{1}{2} \kappa \nabla^2 h^2 + \frac{1}{2} \gamma h^2 \right] \quad (1)$$

that includes the bending and e eective surface tension energy of the bilayer (see for example [14]) in terms of the normal displacement h . The surface tension coefficient arises from the constraint of constant surface area of the bilayer in the closed geometry of the RBC [10, 15]: $\gamma_0 = \gamma - R^2 \kappa \sim 10^9 \text{ J/m}^2$ (taking $R \sim 4 \mu\text{m}$ as the RBC radius, $\kappa \sim 1$). The constant can vary $\sim 1 - 100$.

The last term in (1) is mathematically equivalent to a Lagrange multiplier that constrains the mean square amplitude of bilayer uctuations to be equal to: $\langle h^2 \rangle = k_B T / 8 \kappa$, for an infinite bilayer. This term describes the e eect of the cytoskeleton on the bilayer through a harmonic potential that maintains an average separation d (of order w) between the lipid bilayer and the

cytoskeleton [14], here treated as a separated, infinitely rigid shell, that does not participate in the thermal fluctuations. The discrete contacts that maintain the constant average separation are not specifically described in this continuum model; in a coarse-grained picture, these contacts are the physical origin of the constraint (potential) that determines the average membrane-spectrin network separation.

The attachment of the cytoskeleton to the bilayer also causes stretching and undulations of the bilayer [16], partly due to steric repulsion between the spectrin and the bilayer around the point of attachment [17]. Balancing the spectrin stretching with a local curvature of the bilayer, results in a membrane with undulations of wavelength [16, 18] $L = 100 - 200 \text{ nm}$ and amplitude 10 nm (w) [1, 13]. In our conning-shell model this length-scale is related to the potential-induced persistence length of the bilayer $\ell_0 = (\kappa/\sigma)^{1/4} L$ [14], i.e. the wavelength below which the bilayer is freely fluctuating.

We now calculate the spatial correlations for a two-dimensional, flat bilayer, since for all but the largest wavelengths, the surface of the RBC is relatively flat: $50 \text{ nm} < \lambda < 1 \mu\text{m} < R = 4 \mu\text{m}$. We determine the values of κ and σ by fitting to the experimental data. From Eq. (1) the equal-time (static) correlations of the normal deflections of the bilayer can be written [8, 14]

$$\langle h_q h_{-q} \rangle = \frac{k_B T}{q^4}; \quad \langle h_q \rangle = \langle h_{-q} \rangle = 0 \quad (2)$$

In the inset of Fig.1 we plot the measured value of $\langle h_q \rangle$ in the form $\langle h_q \rangle = \langle h_{-q} \rangle$ as a function of the normalized wavevector $(qd)^4$ (where d is determined by fitting the data to obtain $\langle h_q \rangle / d^4$). From the linear slope in the limit of $q \rightarrow 0$ we find the values of the parameter $\sigma = 7.5; 1.0 \cdot 10^7 \text{ J/m}^2$, for the two cells measured. These values correspond to mean amplitudes $d = 200; 350 \text{ \AA}$ and $\ell_0 = (\kappa/\sigma)^{1/4} = 130; 220 \text{ nm}$ respectively. At larger values of q there is a noticeable deviation from a straight line, which arises from the effective surface tension $\sigma = 7.7; 2.8 \cdot 10^7 \text{ J/m}^2$ for the two cells. Note that surface tension alone, without the conning effect of the cytoskeleton (i.e. $\sigma = 0$), does not fit the data (dash-dot line, Fig.1 inset). In addition, there is a rather abrupt change at the crossover wavevector $q_0 = 1/\ell_0$ (indicated by the vertical dashed lines in Fig.1), above which the data are better described using $\sigma = 1.4 \cdot 10^9 \text{ J/m}^2$ (solid lines in Fig.1).

The measured surface tension is consistent with: $\sigma = \sigma_0$ (of order $\sigma_0 = 10$). This expression gives the effect of bilayer shape constraint due to the static undulations of lateral size $\ell_0 = \ell_0$, described above. Indeed at length-scales shorter than ℓ_0 , there is no stretching of the cytoskeleton (Fig.1). Note that the effective surface tension of a closed bilayer is a very sensitive function of the excess area of the bilayer [10, 19], which is affected by the induced undulations. The spread in the measured

parameters may be due to natural variations in the cytoskeleton network of normal RBC cells.

There is a qualitative difference in power-law of the wavevector dependence of $\langle h_q \rangle$ for RBC and empty vesicles [15]. The vesicles are well described (Fig.2) by equations (1,2) with $\sigma = 0$, and an effective surface tension: $\sigma_{\text{vesicle}} = \kappa/R^2 = 2 \cdot 10^{10} \text{ J/m}^2$, where $R = 27 \mu\text{m}$ and $\kappa = 1.3 \cdot 10^{19} \text{ J}$ are the vesicle radius and bending modulus respectively. Both the RBC's and vesicles data collapse when the wavelength is scaled by the rms amplitude d (Fig.2). For the vesicles of diameter $50 \mu\text{m}$ [15] the rms thermal amplitudes are $d = 1 - 1.5 \mu\text{m}$ (note that here d is not related to conningment). The good scaling of the data indicates that there is indeed a single important length-scale in the problem, namely the persistence length ℓ_0 , that determines all the parameters appearing in the free energy (κ and σ) and the rms amplitude d .

We now use the same simple model of spectrin conningment of the bilayer to describe the temporal correlations of the membrane fluctuations. The shape fluctuations of the RBC membrane are driven by both thermal and metabolic energies. The active fluctuations have a frequency spectrum that is confined to the range $0.3 - 1 \text{ Hz}$ [20]. For higher frequencies, our analysis shows that the active processes can be accounted for by an increase in the effective temperature of the fluctuations [20, 21]. The temporal height-height correlation function [7, 22] for a bilayer at a distance D_1 from a rigid wall, is

$$\langle h_q(t) h_{-q}(0) \rangle = \frac{k_B T}{q^4} e^{-\gamma(q)t} \quad (3)$$

where $\gamma(q)$ is given in (2). The hydrodynamic interaction (Oseen interaction kernel [23]) has a modified form: $\gamma(q) = (1 + 2qD_1) / (1 + 2qD_1) e^{-2qD_1}$; $\gamma(q) = 1 + 4q$ for a free bilayer, so that the relaxation frequency $\gamma(q)$ is

$$\gamma(q) = \frac{1}{4} q^3 + q + \frac{1}{q} (1 + 2qD_1) e^{-2qD_1} \quad (4)$$

where η_{water} is some average viscosity of the cytoplasm and external solution. In the limit of short wavelengths ($q \rightarrow 1$) we recover the free bilayer frequency: $\gamma(q) \rightarrow q^3 = 4$.

The mean square amplitude of the normal fluctuations, as a function of frequency γ , is the Fourier transform

$$\begin{aligned} d(\gamma)^2 &= \frac{1}{(2\pi)^2} \int_0^\infty \int_0^\infty q dq \langle h_q(t) h_{-q}(0) \rangle e^{-i\gamma t} dt \\ &= \frac{1}{(2\pi)^2} \int_0^\infty \langle h_q(0) h_{-q}(0) \rangle \frac{\gamma(q)}{\gamma(q)^2 + \gamma^2} q dq \quad (5) \end{aligned}$$

For a free bilayer this expression (5) gives an anomalous frequency dependence [22]: $d(\gamma)^2 / \gamma^5 = 3$. We integrate the expression (5) numerically in the range $\sigma R < q < \sigma a$ ($a = 50 \text{ \AA}$), and compare with the experimental data [20]. In the inset of Fig.3 we plot $d(\gamma)$

using the parameters of the two cells of Fig.1, and both the high and low values of the effective surface tension (γ and γ_0 respectively). We find a reasonable agreement between the calculation and the measurements, when taking $D_1 = 0.4d$. The similar magnitude of the bilayer-rigid shell separation from both static and dynamic experiments, shows the overall consistency of our confinement model.

In the limit of high frequencies, the earlier result of Brochard et al. [7], gave $d(\omega)^2 / \omega^4 = 3$. Since $qD_1 = 1$ in the measured range, we find in this limit (4): $d(\omega)^2 / \omega^4 = 4$, leading to $d(\omega)^2 / \omega^4 = 5$. It is difficult to distinguish between these two values using the newer data [20]. Our calculation has the advantage of consistently describing both the static (spatial) and dynamic (temporal) fluctuation data. Note that the case of a pure bilayer with large effective surface tension, but without the effect of the rigid wall, is in complete disagreement with the data (dotted line, Fig.3 inset).

In Fig.3 we show that the normal RBC, ATP depleted RBC and RBC ghost, are all well described by the same expression (5) (using the softer cell from Fig.1, i.e. the smaller γ and γ_0), differing by an effective temperature factor of up to 3. This is similar to the amplitude enhancement factor of 2.5 found in a previous study [21].

The largest effect of the rigid shell is to increase the effective viscosity of the water near the bilayer, by constraining its flow. Defining an effective viscosity by: $\eta_{eff} = \eta q^3 = 4\eta_{eff}$, we get from (4): $\frac{\eta_{eff}}{4d^2(\frac{1}{\gamma} + \frac{1}{\gamma_0})} = \frac{q^2}{4d^2(\frac{1}{\gamma} + \frac{1}{\gamma_0})}$. At the crossover wavevector q_0 this function has its peak: $\eta_{eff} = 45 \times 30$, depending on the value of γ . These values are in close agreement with the value $\eta_{eff} = 50$ found from the relaxation times of an electrodeformed RBC [3, 5]. In these experiments, the cytoplasm flows through the cytoskeleton mesh, setting up a flow field

at the crossover wavevector q_0 . Thus, a rigid cytoskeletal wall, separated by a fixed distance from the bilayer, accounts for the larger effective viscosity required to fit these dynamical experiments.

While this model accounts for the wavevector dependence of the statics and the frequency dependence of the dynamics, the absolute amplitude of the fluctuations and the different values observed in active and ATP-depleted cells, must still be explained. One possibility is that ATP driven fluctuations completely determine the amplitude of the largest wavelength fluctuations [20] through the process of spectrin-actin disconnections and reconnections [1, 11, 20]. These ATP-driven conformational changes give rise to defects in the triangular spectrin network, resulting in nodes with more or less than 6 spectrin bonds. The local curvature of the cytoskeleton may change at the site of a defect, from being locally flat (6 bonds) to having a 80nm deviation out of the plane of the flat cytoskeleton (5-fold node). The effect of this random buckling is to increase the mean bilayer-rigid shell separation by a factor of 4. According to our model, this will increase the amplitude of the $q \rightarrow 0$ modes by a factor of 4, as measured [5].

Acknowledgments

We thank R. Korenstein, E. Sackmann and H. Strey for useful discussions. This work was supported by the ISF grant for Center on Self-Assembly. The authors are grateful to the donors of the Petroleum Research Fund administered by the American Chemical Society and to the Schmidt Minkowski Center for their support. N.G.'s research is being supported by the Louis L. and Anita M. Perlman Postdoctoral Fellowship.

-
- [1] H. Strey, M. Peterson and E. Sackmann, *Biophys. J.* 69 (1995) 478.
 - [2] D. Discher, N. Mohandas and E. A. Evans, *Science* 266 (1994) 1032; V. Heinrich, K. Ritchie, N. Mohandas, and E. Evans, *Biophys. J.* 81 (2001) 1452.
 - [3] H. Engelhardt, H. Gaub and E. Sackmann, *Nature* 307 (1984) 378.
 - [4] E. Sackmann, *FEBS Letters* 346 (1994) 3.
 - [5] M. A. Peterson, *Phys. Rev. A* 45 (1992) 4116.
 - [6] J.-C. M. Lee and D. E. Discher, *Biophys. J.* 81 (2001) 3178.
 - [7] F. Brochard and J. F. Lennon, *J. de Physique* 36 (1975) 1035.
 - [8] M. Peterson, H. Strey and E. Sackmann, *J. Phys. II France* 2 (1992) 1273.
 - [9] A. Zilker, H. Engelhardt and E. Sackmann, *J. de Physique* 48 (1987) 2139.
 - [10] U. Seifert and R. Lipowsky, *Structure and Dynamics of Membranes, Vol.1A*, p.403, Eds: R. Lipowsky and E. Sackmann, *Elsevier* (1995).
 - [11] V. Bennett, *Biochim. Biophys. Acta* 988 (1989) 107.
 - [12] E. Sackmann, *Structure and Dynamics of Membranes, Vol.1A*, p.1, Eds: R. Lipowsky and E. Sackmann, *Elsevier* (1995).
 - [13] L. D. Landau and E. M. Lifshitz, *Theory of Elasticity*, Pergamon Press (1981); A. H. Swihart, J. M. Mikkut, J. B. Ketterson and R. C. Macdonald, *J. Microscopy* 204 (2001) 212; S. K. Boey, D. H. Boal and D. E. Discher, *Biophys. J.* 75 (1998) 1573.
 - [14] S. A. Safran, *Statistical Thermodynamics of Surfaces, Interfaces and Membranes*, *Frontiers in physics* v.90, Addison-Wesley Publishing Company (1994).
 - [15] W. Hackl, U. Seifert and E. Sackmann, *J. Phys. II France* 7 (1997) 1141.
 - [16] K. Zeman, H. Engelhardt and E. Sackmann, *Euro. Biophys. J.* 18 (1990) 203.
 - [17] M. Breidenich, R. R. Netz and R. Lipowsky, *Europhys. Lett.* 49 (2000) 431; R. Lipowsky, H.-G. Dobereiner, C. Hiergeist and V. Indrani, *Physica A* 249 (1998) 536.
 - [18] Another way to derive the amplitude of the spontaneous bilayer undulations is to compare the steric repulsion of

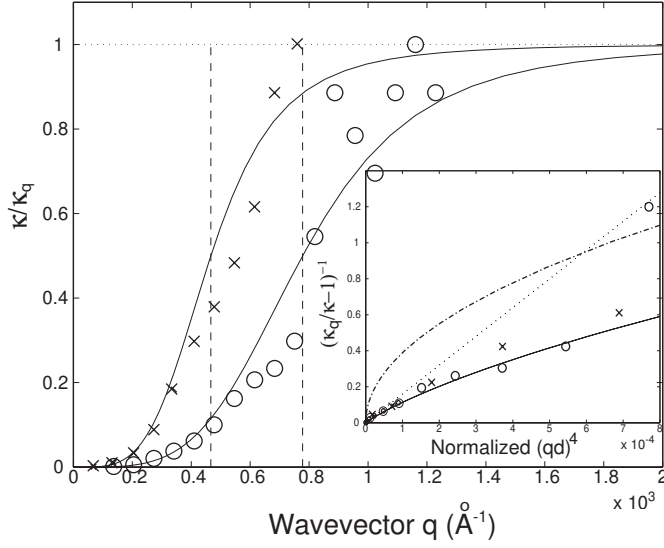


FIG. 1: The calculated (Eq. 2) wavevector dependence of the bending modulus κ_q of the RBC (solid lines, taking $\kappa = \kappa_0$) compared with the experimental data for the RBC [9] (o,x). The crossover wavevector q_0 is indicated by the vertical dashed lines. Inset: A plot of $(\kappa_q/(\kappa-1))^{-1}$ as a function of the normalized wavevector $(qd)^4$ for small wavevectors. The linear slope in the limit of $q \rightarrow 0$ is indicated by the dotted line. The deviation from linear behavior is well described by an effective surface tension $\gamma = 2.8; 7.7 \times 10^{-7} \text{ J/m}^2$ for the two cells (solid line). Note that surface tension alone, without conning wall ($\kappa = 0$), does not describe the data (dash-dot line).

the bilayer thermal fluctuations per area with the areal modulus of the cytoskeleton: $\gamma = (\kappa_B T)^2 = d^2 \kappa$ [see J.O. Radler, T.J. Feder, H.H. Strey and E. Sackmann, Phys. Rev. E. 51 (1995) 4526].

- [19] P. Sens and S.A. Safran, Europhys. Lett. 43 (1998) 95.
- [20] S. Tuval, S. Levin, A. Bitler and R. Korenstein, J. of Cell Bio. 141 (1998) 1551; S. Levin and R. Korenstein, Biophys. J. 60 (1991) 733.
- [21] J.-B. Manneville, P. Bassereau, D. Levy and J. Prost, Phys. Rev. Lett. 82 (1999) 4356.
- [22] A.G. Zilman and R.G. Granek, Phys. Rev. Lett. 77 (1996) 4788.
- [23] L.D. Landau and E.M. Lifshitz, Fluid Mechanics, Pergamon Press (1987); A. Zilman and R. Granek, in preparation.

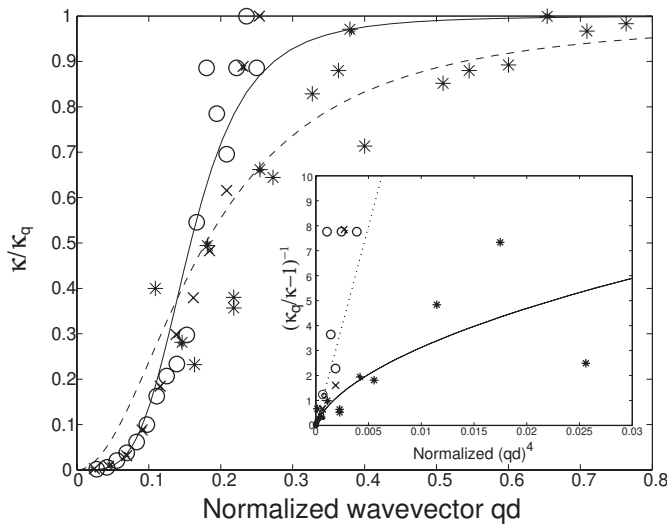


FIG. 2: A plot of the the measured effective modulus κ/κ_q of RBC [9] (o,x) and empty giant vesicles [15] (*) as a function of the normalized wavevector qd . The calculations are given by the solid and dashed line respectively. Inset: A plot of $(\kappa_q/\kappa - 1)^{-1}$ as a function of the normalized wavevector $(qd)^4$ for small wavevectors. The linear slope in the limit of $q \rightarrow 0$ for the RBC is indicated by the dotted line. The calculation for the vesicle is given by the solid line.

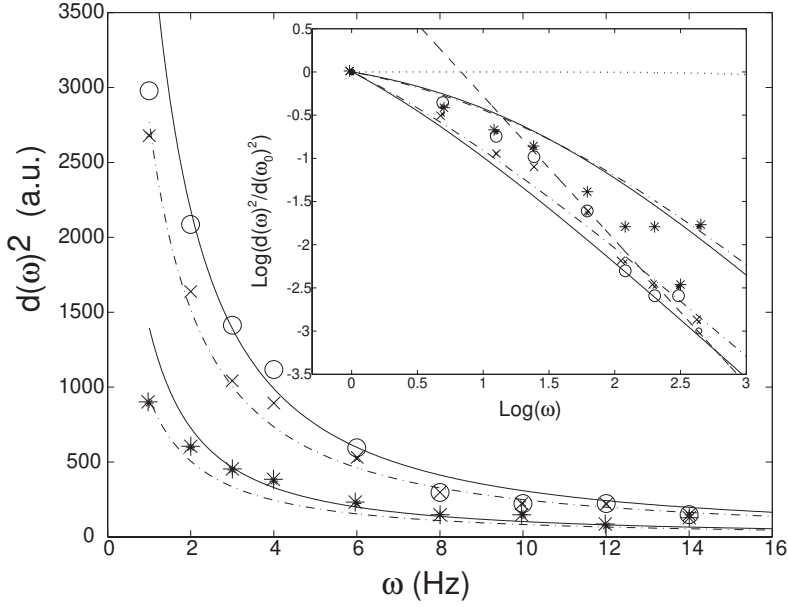


FIG. 3: Frequency dependence of the mean-square amplitude $d(\omega)^2$ of the RBC (o), showing the reduction in the amplitude due to partial ATP depletion (x) and complete absence (RBC ghost) (*). The lines of the calculation (Eq. 5) differ by the effective temperature enhancement factor of 3 (solid lines: 0, dash-dot lines: 3). Inset: A normalized Log-Log plot showing the powerlaw dependence ($l_0 = 1 \text{ Hz}$). The calculation is done using the parameters of the two cells of Fig. 1 (solid lines: 0, dash-dot lines: 3). The dashed line shows the free bilayer behavior $d(l)^2 / l^{5=3}$. The case of a free bilayer with large effective surface tension, but without the effect of the rigid wall, is in complete disagreement with the data (dotted line).